




Effects of Silk-Elastin and SpheroSeev Mixture and Minced Cartilage on Cartilage Repair in Rabbit Osteochondral Defect Models

Naofumi Hashiguchi,* MD, MPH , Tomoyuki Nakasa,*[†] MD, PhD, Masakazu Ishikawa,[‡] MD, PhD , Shingo Kawabata,[§] Shunya Tsuji,* MD, Atsuo Nakamae,* MD, PhD , Shigeru Miyaki,^{||} PhD, and Nobuo Adachi,* MD, PhD

Investigation performed at the Department of Orthopaedic Surgery, Graduate School of Biomedical & Health Sciences, Hiroshima University, Hiroshima, Japan

Background: Autologous chondrocyte implantation, a 2-stage, costly procedure, has limitations, prompting the development of 1-step techniques utilizing autologous minced cartilage (MC). However, novel scaffolds for cell migration and proliferation are needed to enhance their effectiveness.

Purpose: To evaluate the effectiveness of silk-elastin and SpheroSeev (SESS) scaffolds in enhancing chondrocyte activity and promoting cartilage repair in a rabbit model of osteochondral defect repair.

Study Design: Controlled laboratory study.

Methods: The effects of a SESS mixture combined with MC on cartilage repair in osteochondral defects were investigated in 42 Japanese White rabbits, with the defect (Df) group serving as the control. Bilateral osteochondral defects were created in the knees of 36 rabbits, treated with MC, SESS, and a combination of MC and SESS, with all treated sites sealed using fibrin glue. Osteochondral cartilage repair was evaluated using the modified O'Driscoll histological scoring, immunohistochemistry for collagen type II expression, and Ki67 staining for cell proliferation at 8, 12, and 24 weeks postoperatively.

Results: SESS alone and in combination with MC significantly enhanced osteochondral cartilage repair in the rabbit models by 24 weeks compared with the Df group ($P < .05$). Among them, histological scoring was higher in the SESS group (20.7 ± 6) than in the Df and MC groups (8.8 ± 6.7 , $P = .046$; 7.8 ± 5.7 , $P = .023$). This resulted in smooth surfaces and histological features similar to normal cartilage. Immunohistochemical analyses revealed improved repair quality with increased expression of type II collagen and Ki67, indicating superior repair and cellular activity relative to the controls.

Conclusion: The combined use of SESS and MC effectively promoted cartilage repair in rabbit osteochondral defects. Notably, the SESS mixture appears to enhance the structural and compositional repair of cartilage tissue, offering a promising approach for the treatment of osteochondral defects.

Clinical Relevance: The novelty of this approach lies in combining silk-elastin and recombinant spider silk fibers, both of which provide mechanical support and promote cell proliferation, making them promising candidates for enhancing cartilage repair in osteochondral defects. Utilizing the SESS mixture as a scaffold for cartilage repair in osteochondral defects offers a 1-step, cost-effective alternative to traditional autologous chondrocyte implantation, potentially enhancing cartilage repair and improving tissue structure and biochemistry.

Keywords: autologous chondrocyte implantation; minced cartilage; osteochondral defect; silk-elastin and SpheroSeev

Autologous chondrocyte implantation has proven effective in the treatment of bone and cartilage defects, yielding positive clinical outcomes.^{2,5,7} However, it has several drawbacks—including invasiveness, cost, and the need for a 2-stage procedure involving cartilage harvesting and subsequent chondrocyte cell implantation.⁹ To address these

challenges, 1-step surgeries utilizing autologous minced cartilage (MC) have emerged,^{6,25} offering reduced invasiveness, cost-effectiveness, and promising therapeutic potential.¹² Recently, combining MC with scaffolds has shown promise in enhancing chondrocyte migration, proliferation, and cartilage matrix production, marking a significant advancement in regenerative medicine.³⁵ For instance, Matsushita et al²⁸ demonstrated the efficacy of MC implantation combined with atelocollagen gel for treating osteochondral defects in rabbits, suggesting its viability as an alternative to conventional autologous chondrocyte implantation.

The selection of appropriate scaffolding material is crucial in 1-step surgery procedures for fixing MC tissue in the bone-cartilage defect site, as they significantly influence tissue repair and clinical outcomes.^{24,30,33,36} Previous studies have highlighted silk fibroin, the precursor to silk-elastin, for promoting cartilage repair by serving as a scaffold for cartilage tissue formation.^{4,8,18} Similarly, recombinant spider silk fibers (SpheroSeev, Seevix Material Sciences Ltd) have emerged as another promising option for cartilage repair, owing to their biocompatibility and support for chondrocyte growth.^{32,34} The transition of SpheroSeev from solid to fluid states, coupled with silk-elastin, holds promise for effective cartilage repair. Research has suggested that the synergy between these materials, given their biological and mechanical properties, presents an attractive avenue for cartilage defect repair.^{13,22}

Consequently, this study aimed to investigate 2 scaffolding materials: silk-elastin protein and recombinant spider silk fibers. Silk-elastin, an artificial protein synthesized via genetic recombination, mimics natural proteins like elastin and silk fibroin.¹⁷ Because of its high cell affinity and elasticity, silk-elastin is considered suitable for treating wounds.²⁹ Silk-elastin can form a gel in solution by swelling at higher temperatures, facilitating water incorporation into its structure. Therefore, this study aimed to evaluate the effectiveness of MC implantation with the silk-elastin and SpheroSeev (SESS) scaffold in repairing cartilage defects. We hypothesized that combining MC with a scaffold comprising SESS would enhance cartilage repair by harnessing the advantages of both materials.

METHODS

Animals

All procedures were performed in accordance with the guidelines for animal experimentation at our institution

TABLE 1
Distribution of Animals by Treatment of Limbs
and Histologic Evaluation Time^a

	8 Weeks	12 Weeks	24 Weeks
Df: SESS	6	6	6
MC: MCSESS	6	6	6

^aDf, defect; MC, minced cartilage; MCSESS, minced cartilage and silk-elastin and SpheroSeev; SESS, silk-elastin and SpheroSeev.

and with the approval of the Committee of Research Facilities for Laboratory Animal Sciences, Graduate School of Biomedical Sciences. A total of 42 male Japanese White rabbits weighing between 2.5 and 3 kg were utilized in this study. Surgeries were conducted under general anesthesia induced by ketamine hydrochloride and xylazine. To evaluate the effects of the SESS scaffold on osteochondral repair, osteochondral defect models were established in both the knees of 36 rabbits according to previous research²⁷ (Table 1). The patellae were laterally dislocated via the medial parapatellar approach. Defect sites were marked using a 5-mm diameter biopsy punch and drilled with a 2.3-mm diameter drill bit attached to a microgrinder (Minitor's Premo 25S2) operating at 10,000 rpm, with continuous irrigation using phosphate-buffered saline (PBS) to prevent heat-induced tissue damage. This procedure produced a circular defect measuring 5 mm in diameter and 3 mm in depth, consistent with previous studies.^{16,27} The defect site was then thoroughly washed with 50 mL of PBS. An additional 6 rabbits were used to harvest articular cartilage from the shoulder and knee joints. Shoulder and knee cartilage were harvested to obtain sufficient chondrocytes, and the harvested tissue was finely minced in a mesh-like pattern using a scalpel to achieve a paste-like consistency, following established protocols for cartilage repair.³ The MC was washed twice with PBS and disinfected by soaking in 500 mL PBS containing 1% antibiotics (5 mg *Amphotericin B*) and centrifuged twice at 400 g for 10 minutes. The defect volume and grafted cartilage fragments were calculated based on previous studies, and the cartilage was manually minced into 8 mg fragments in a petri dish using a scalpel.²⁷ Subsequently, MC was used in vivo. The SESS scaffold was prepared by mixing 15% silk-elastin with 0.25% SpheroSeev to form a hybrid sponge capable of transitioning from solid to gel. Fibrin glue (BOLHEAL

[†]Address correspondence to Tomoyuki Nakasa, MD, PhD, Department of Orthopaedic Surgery, Graduate School of Biomedical & Health Sciences, Hiroshima University, 3-2-1, Kasumi, Minami-ku, Hiroshima city, 734-0037, Japan (email: tnakasa0@gmail.com).

^{*}Department of Orthopaedic Surgery, Graduate School of Biomedical & Health Sciences, Hiroshima University, Hiroshima, Japan.

[‡]Department of Orthopaedic Surgery, Faculty of Medicine, Kagawa University Hospital, Japan.

[§]Sanyo Chemical Industries, LTD, Japan.

^{||}Medical Center for Translational and Clinical Research, Hiroshima University Hospital, Japan.

Final revision submitted November 14, 2024; accepted December 17, 2024.

The authors have declared that there are no conflicts of interest in the authorship and publication of this contribution. AOSSM checks author disclosures against the Open Payments Database (OPD). AOSSM has not conducted an independent investigation on the OPD and disclaims any liability or responsibility relating thereto.

Ethical approval for this study was obtained from Hiroshima University (A22-201).

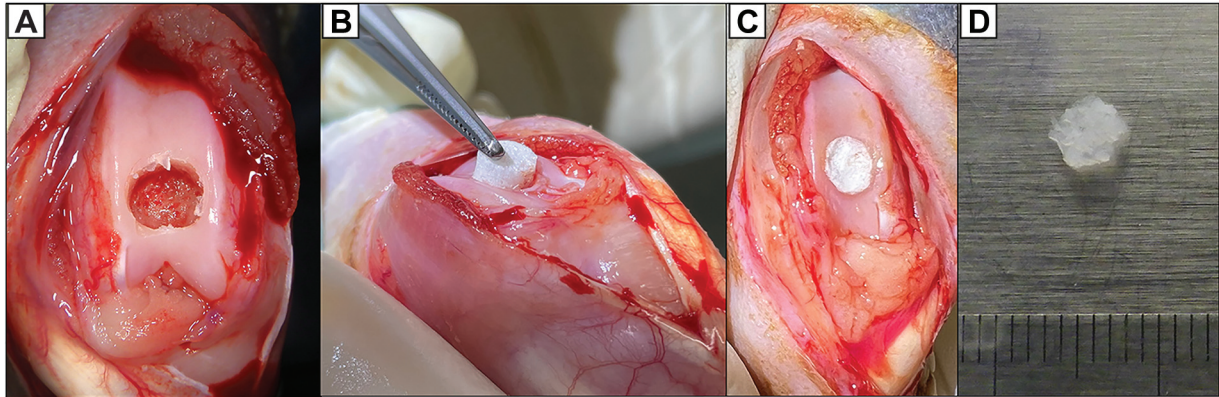


Figure 1. Experimental photos. (A) A 5-mm diameter and 3 mm deep defect. (B) Dried transplant site with solid SESS embedded. (C) SESS embedded into the defect. (D) An 8-mg piece of cartilage. SESS, silk-elastin and SpheroSeev.

Tissue Sealant; KM Biologics) was applied to all groups as a sealing agent. In the MC group, 8 mg of MC was inserted into the defect before applying fibrin glue. In the SESS group, a solid SESS gel (5 mm in diameter and 3 mm deep) was implanted into the defect before fibrin glue application (Figure 1). For the combined MC and SESS (MCSESS) groups, 8 mg of MC was first implanted into the defect, followed by the SESS scaffold, and then sealed with fibrin glue. A small amount of fibrin glue (0.5 mL) was prepared and applied to fill the defect. The joint capsule and skin were sutured using 5-0 and 4-0 nonabsorbable nylon sutures (Bear Medic Corporation), respectively.

Histological Evaluation

At 8, 12, and 24 weeks postoperatively, the rabbits were euthanized using carbon dioxide. At each time point, 6 knees (femur and patella) from each group were evaluated. The patella was included in the analysis because it articulates directly with the femoral trochlea, where the osteochondral defects were created. This allows for the evaluation of potential secondary effects of treatment on adjacent cartilage structures. Knee joints were harvested and fixed with 4% paraformaldehyde at 4°C overnight. After 4 to 6 weeks of decalcification in neutral decalcification liquid EDT-X (FALMA), the samples were embedded in paraffin, and 4 μ m thick sections were prepared. Safranin O/Fast Green staining was performed on the femur and patella. The modified O'Driscoll histological scoring scale, ranging from 0 (worst) to 27 (best), was used for semiquantitative analysis of the femur.³¹ This scoring system evaluates cartilage repair quality by assessing tissue characteristics, structural features, and degenerative changes. The investigation of patellar cartilage was included because of its direct contact with the femoral trochlea, where the osteochondral defect was located, allowing us to assess the indirect effects of treatment on adjacent cartilage. The Osteoarthritis Research Society International (OARSI) score, ranging from 0 (best) to 25 (worst), was used for semiquantitative analysis of the patella.²¹ The OARSI system evaluates osteoarthritis

severity by assessing cartilage depth changes and joint surface involvement. Histological grading was performed by 2 observers (G.K. and J.T.) who were blinded to the source of the samples.

Immunohistochemistry

The sections underwent pretreatment with an antigen retrieval reagent (Immunoactive; Matsunami Glass Ind) overnight for heat activation, followed by treatment with 3% hydrogen peroxide for 10 minutes, normal blocking serum for 30 minutes, and incubation with primary antibodies against type II collagen (dilution 1:100; anti-hCL [II]; Daiichi Fine Chemical), type I collagen (dilution 1:250; Novus Biologicals), and Ki67 (dilution 1:400; Cell Signaling Technology) overnight at 4°C. The following day, the sections were visualized using the avidin-biotin system (Vectastain Elite ABC Mouse IgG kit; Vector Laboratories Inc) and 3,3'-diaminobenzidine (Peroxidase Substrate Kit; Vector Laboratories Inc), according to the manufacturer's instructions.

The immunohistochemical expression of chondrocyte cells in the femur was evaluated using the integrated optical density (IOD).²³ The IOD is measured in pixels per area and allows for the estimation of the relative amount of the target object in the background of the image. Ten areas (300 \times 300-mm grid) in the region of interest on the cartilage surface of each section were randomly selected, and IOD values were measured using ImageJ 1.53 software. For semiquantitative analyses, the data were expressed as the mean IOD (IOD/area).³⁹ To assess chondrocyte migration and proliferation in the subchondral bone after implantation, 3 areas (300 \times 300-mm grid) in the reparative tissue of each section were randomly selected, and cells were counted under 400 \times magnification. The mean number of Ki67-positive cells per area was calculated for each group, as previously described.²⁷

Statistical Analysis

Data were presented as the standard error of the mean. Statistically significant differences in the Modified

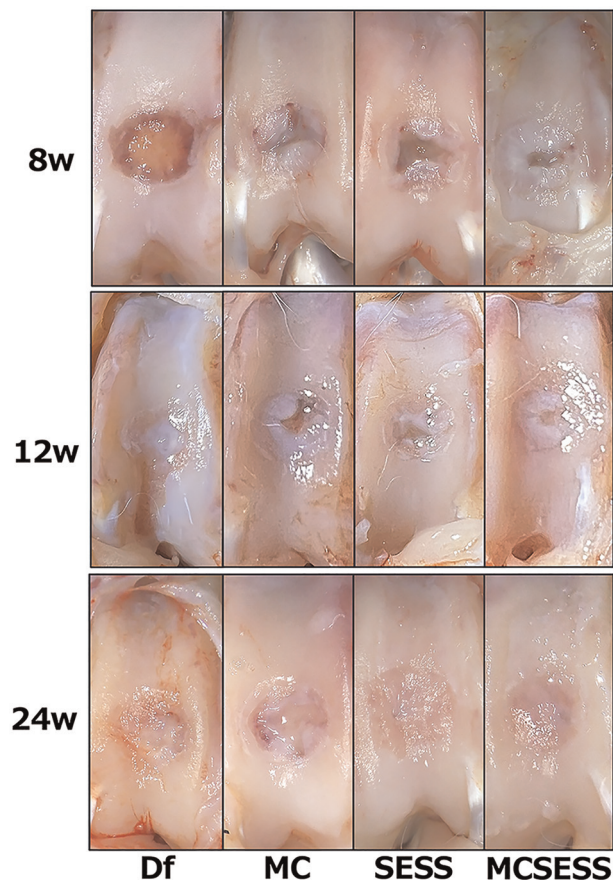


Figure 2. Gross appearance in each group at 8, 12, and 24 weeks postoperation. Df, defect; MC, minced cartilage; MCSESS, minced cartilage and silk-elastin and Sphero-Seev; SESS, silk-elastin and SpheroSeev.

O'Driscoll histological scoring scale, OARSI scores, IOD values, and Ki67-positive cell rates among the 4 treatment groups were evaluated using the Kruskal-Wallis test followed by the Dunn multiple comparison test, with a significance level set at $P < .05$. All analyses were conducted using GraphPad Prism 10.2 for Mac (GraphPad Software Inc).

RESULTS

Gross Appearance

At 8 weeks postoperation, the defect (Df) group exhibited minimal repaired tissue in the defect area, whereas the other 3 groups (MC, SESS, and MCSESS) showed gradual formation of white fibrous tissue originating from the edges. Except for the Df group, the edges of the tissues in these 3 groups were smooth (Figure 2).

By 12 weeks, the osteochondral defect area in the Df group was filled with white fibrous tissue, with edge degeneration progressing to bone sclerosis. Conversely, the other 3 groups demonstrated an increased coverage

of white fibrous tissue in the transplanted areas compared with the 8-week mark, with a gradual decrease in defect size (Figure 2).

At 24 weeks postoperation, the Df group displayed irregular surfaces with indentations. Similarly, in the MC group, the center of the defect was filled with fragile tissue that was not fibrous, resulting in an irregular surface. Both the SESS and MCSESS groups exhibited a glossy, smooth surface, with fibrous tissue seamlessly integrating with the adjacent cartilage. No enlargement of repaired tissue or synovitis was observed throughout the observation period (Figure 2).

Histological Evaluation

Femur. At 8 weeks postoperatively, the osteochondral defect was barely filled in the Df group. In contrast, reparative tissue with Safranin O-positive areas appeared within the defects in the other 3 groups. The MC group showed fewer defect fillings compared with the 2 groups using SESS. MC fragments were observed beneath the subchondral bone in the MC group, where subchondral bone formation had begun. Bone marrow formation and chondrocyte proliferation were evident in the SESS and MCSESS groups, with some MC visible in the MCSESS group (Figure 3).

The modified O'Driscoll histological scoring scale scores at 8 weeks for the MC, SESS, and MCSESS groups were higher than those for the Df group, however, the differences were not statistically significant (Table 2). Furthermore, the scores in the SESS group varied widely (Figure 4).

At 12 weeks postoperatively, no cartilage tissue was observed in the defective area in the Df group. In the MC group, chondrocytes in the Safranin O-positive area were sparse, and subchondral bone formation was minimal. In the SESS group, despite sparse chondrocytes in the Safranin O-positive area, bone marrow formation was observed. The MCSESS group exhibited more chondrocytes in the Safranin O-positive area than the other groups, with good bone marrow formation and a smooth cartilage surface (Figure 3).

At 12 weeks postoperation, the modified O'Driscoll histological scoring scale scores for the SESS and MCSESS groups were significantly higher than those for the Df group (Df vs SESS, $P = .0097$, Df vs MCSESS, $P = .019$) (Table 2 and Figure 4).

At 24 weeks postoperation, the Df group still had a remaining defect with almost no Safranin O-positive chondrocytes. In the MC group, minced cartilage fragments persisted, but Safranin O-positive chondrocytes were sparse, and the osteochondral junction was poorly reconstructed. The SESS group showed a thinner defect with Safranin O-positive chondrocytes present, although Safranin O-negative fibrous tissue was also observed on the surface. The subchondral bone was repaired to the level of the surrounding subchondral bone. In the MCSESS group, the articular cartilage was close to normal thickness with abundant chondrocytes in the Safranin O-positive area, although the cartilage surface remained irregular.

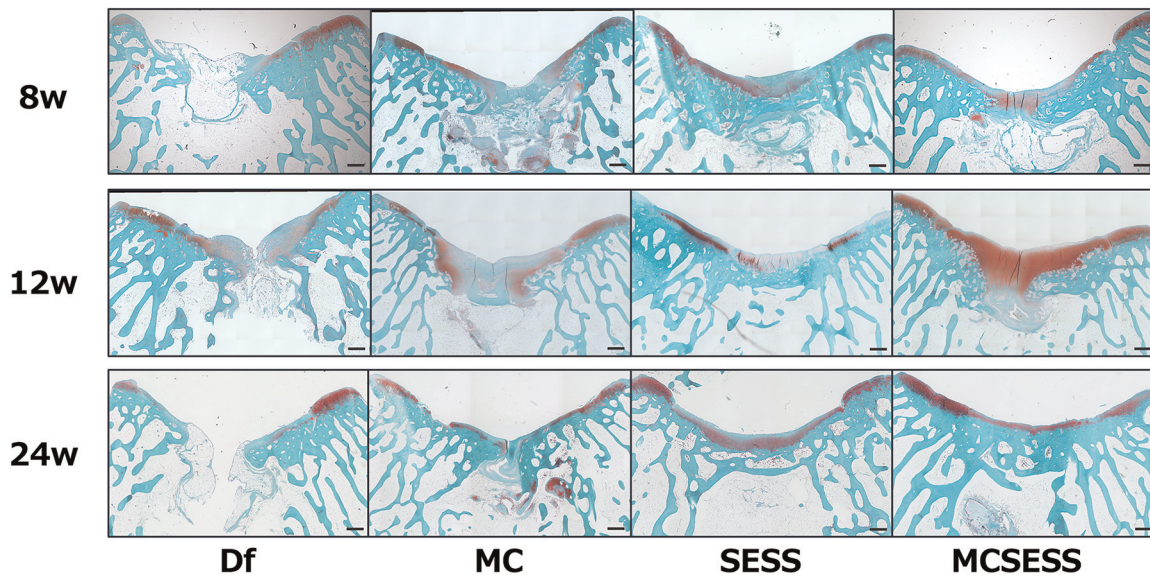


Figure 3. Safranin O/Fast Green staining for the femur in each group at 8, 12, and 24 weeks postoperation. Scale bar: 500 mm. Df, defect; MC, minced cartilage; MCSESS, minced cartilage and silk-elastin and SpheroSeev; SESS, silk-elastin and SpheroSeev.

TABLE 2
Histological and Immunohistochemical Results at 8, 12, and 24 Weeks After Surgery^a

Test and Sacrifice Time in Weeks	Df	MC	SESS	MCSESS
Modified O'Driscoll				
8	7.4 ± 6.3	12.3 ± 4.3	13.1 ± 7.4	16.3 ± 5.8
12	5.8 ± 4.8	13 ± 3.8	17.7 ± 5.3	16.3 ± 4
24	8.8 ± 6.7	7.8 ± 5.7	20.7 ± 6	20.3 ± 3.4
OARSI score				
8	10.8 ± 7.1	10.2 ± 5.2	2.5 ± 2.4	1.7 ± 0.8
12	10.3 ± 6	5.5 ± 3.1	3.2 ± 2	0.83 ± 0.8
24	9.0 ± 6.7	8.2 ± 6.1	2.7 ± 4.6	2.3 ± 2.9
IOD/area, type I collagen				
8	0.43 ± .0.3	0.40 ± 0.06	0.39 ± 0.05	0.33 ± 0.06
12	0.39 ± 0.02	0.41 ± 0.04	0.34 ± 0.01	0.35 ± 0.02
24	0.46 ± 0.05	0.40 ± 0.01	0.34 ± 0.02	0.34 ± 0.02
IOD/area, type II collagen				
8	0.33 ± 0.02	0.35 ± 0.02	0.41 ± 0.06	0.40 ± 0.04
12	0.34 ± 0.009	0.39 ± 0.03	0.41 ± 0.04	0.41 ± 0.05
24	0.35 ± 0.03	0.39 ± 0.07	0.43 ± 0.03	0.44 ± 0.03
Ki67 positive stains, %				
8	8.9 ± 7	19.2 ± 10.5	31.8 ± 10.7	32.8 ± 9.5

^aData are presented as mean ± SD unless otherwise indicated. Df, defect; IOD, integrated optical density; MC, minced cartilage; MCSESS, minced cartilage and silk-elastin and SpheroSeev; SESS, silk-elastin and SpheroSeev.

The osteochondral junction was better reconstructed in the MCSESS group than in the other groups (Figure 3).

At 24 weeks postoperation, the modified O'Driscoll histological scoring scale scores for the SESS group were significantly higher than those for the Df and MC groups (Df vs SESS, $P = .046$, MC vs SESS, $P = .023$) (Table 2). In addition, the score of the MCSESS group was significantly higher than that of the MC group ($P = .041$) (Figure 4).

Patella. At 8 weeks postoperation, the SESS and MCSESS groups exhibited strong Safranin O positivity and thicker cartilage layers resembling normal patellar cartilage. However, the Df and MC groups showed changes in Safranin O negativity in the cartilage surface and intermediate layers, indicating the onset of degeneration (Figure 5A). The OARSI scores were 10.8 ± 7.1 for the Df group, 10.2 ± 5.2 for the MC group, 2.5 ± 2.4 for the

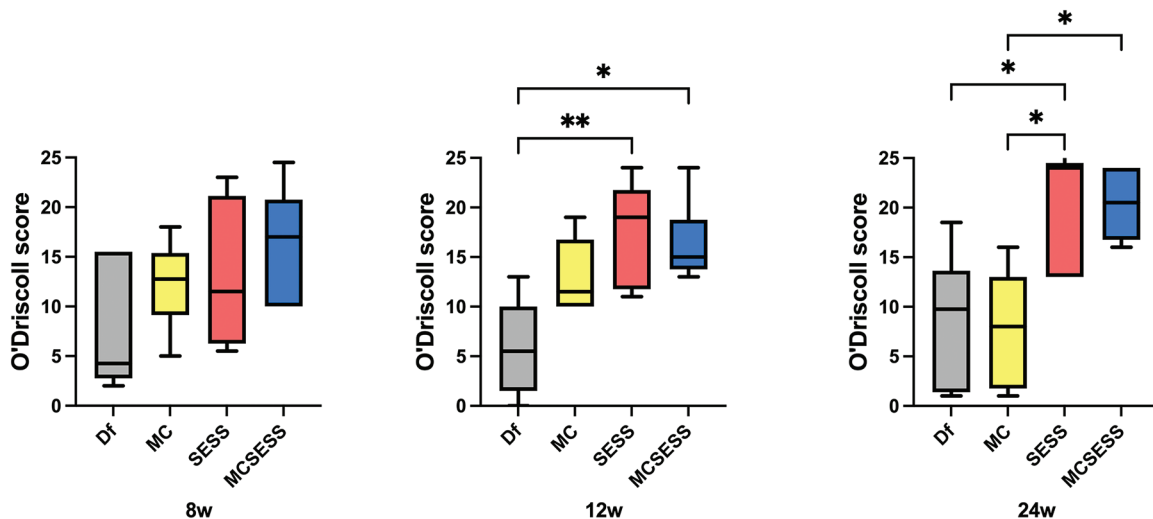


Figure 4. Modification of the O'Driscoll histological scoring scale in each group at 8, 12, and 24 weeks postoperation. * $P < .05$; ** $P < .01$. Df, defect; MC, minced cartilage; MCSESS, minced cartilage and silk-elastin and SpheroSeev; SESS, silk-elastin and SpheroSeev.

SESS group, and 1.7 ± 0.8 for the MCSESS group (Figure 5B). The scores for the MCSESS group were significantly lower than those for the Df and MC groups (Df vs MCSESS, $P = .035$; MC vs MCSESS, $P = .029$) (Table 2).

At 12 weeks postoperatively, the MCSESS group maintained strong Safranin O positivity and thick cartilage layers akin to normal patellar cartilage. The SESS group showed slight degeneration of the cartilage surface layer. The MC group exhibited strong Safranin O negativity on the cartilage surface and intermediate layers, whereas the Df group showed irregularities on the cartilage surface (Figure 5A). The OARSI scores were 10.3 ± 6 for the Df group, 5.5 ± 3.1 for the MC group, 3.2 ± 2 for the SESS group, and 0.83 ± 0.8 for the MCSESS group (Figure 5B). The score for the MCSESS group was significantly lower than that for the Df group ($P < .001$) (Table 2).

At 24 weeks postoperatively, the MCSESS group continued to exhibit strong Safranin O positivity and thick cartilage layers, mirroring normal patellar cartilage. The SESS group showed Safranin O negativity in the cartilage surface layer, indicating slight degeneration and surface irregularities. The MC group showed strong Safranin O negativity in the cartilage surface and intermediate layers, whereas the Df group experienced further degeneration (Figure 5A). The OARSI scores were 9 ± 6.7 for the Df group, 8.2 ± 6.1 for the MC group, 2.7 ± 4.6 for the SESS group, and 2.3 ± 2.9 for the MCSESS group. Although no significant differences were observed, the SESS and MCSESS groups tended to have lower scores (Table 2).

IMMUNOHISTOCHEMISTRY EVALUATION

To further assess bone repair capabilities, immunohistochemical staining for bone and cartilage formation markers was performed. The expression of type I collagen,

a bone formation marker, was detected on the surface of the repaired tissue in the Df group (Figure 6A). At 8 weeks after surgery, the expression levels were as follows: 0.43 ± 0.03 for the Df group, 0.40 ± 0.06 for the MC group, 0.39 ± 0.05 for the SESS group, and 0.33 ± 0.06 for the MCSESS group (Figure 6B). The MCSESS group exhibited significantly lower levels compared with the Df group ($P = .048$) (Table 2). At 12 weeks after surgery, the results were 0.39 ± 0.02 for the Df group, 0.41 ± 0.04 for the MC group, 0.34 ± 0.01 for the SESS group, and 0.35 ± 0.02 for the MCSESS group (Figure 6B). The SESS group showed significantly lower scores compared with the Df and MC groups (Df vs SESS, $P = .026$, MC vs SESS, $P = .011$) (Table 2). By 24 weeks, the results were 0.46 ± 0.05 for the Df group, 0.40 ± 0.01 for the MC group, 0.34 ± 0.02 for the SESS group, and 0.34 ± 0.02 for the MCSESS group (Figure 6B). The SESS and MCSESS groups had significantly lower levels than the Df group (Df vs SESS, $P = .0029$, Df vs MCSESS, $P < .001$) (Table 2).

Furthermore, the expression of type II collagen, a cartilage marker, was assessed via immunohistochemistry (Figure 7A). At 8 weeks postoperatively, the results showed 0.33 ± 0.02 for the Df group, 0.35 ± 0.02 for the MC group, 0.41 ± 0.06 for the SESS group, and 0.40 ± 0.04 for the MCSESS group (Figure 7B). Both the SESS and MCSESS groups exhibited significantly higher values compared with the Df group (Df vs SESS, $P = .033$, Df vs MCSESS, $P = .033$) (Table 2). At 12 weeks, the results were 0.34 ± 0.009 for the MCSESS group, 0.39 ± 0.03 for the MC group, 0.41 ± 0.04 for the SESS group, and 0.41 ± 0.05 for the MCSESS group (Figure 7B). The MCSESS group showed significantly higher levels compared with the Df group ($P = .037$) (Table 2). By 24 weeks, the results were 0.35 ± 0.03 for the Df group, 0.39 ± 0.07 for the MC group, 0.43 ± 0.03 for the SESS group, and 0.44 ± 0.03 for the MCSESS group (Figure 7B). Both the SESS

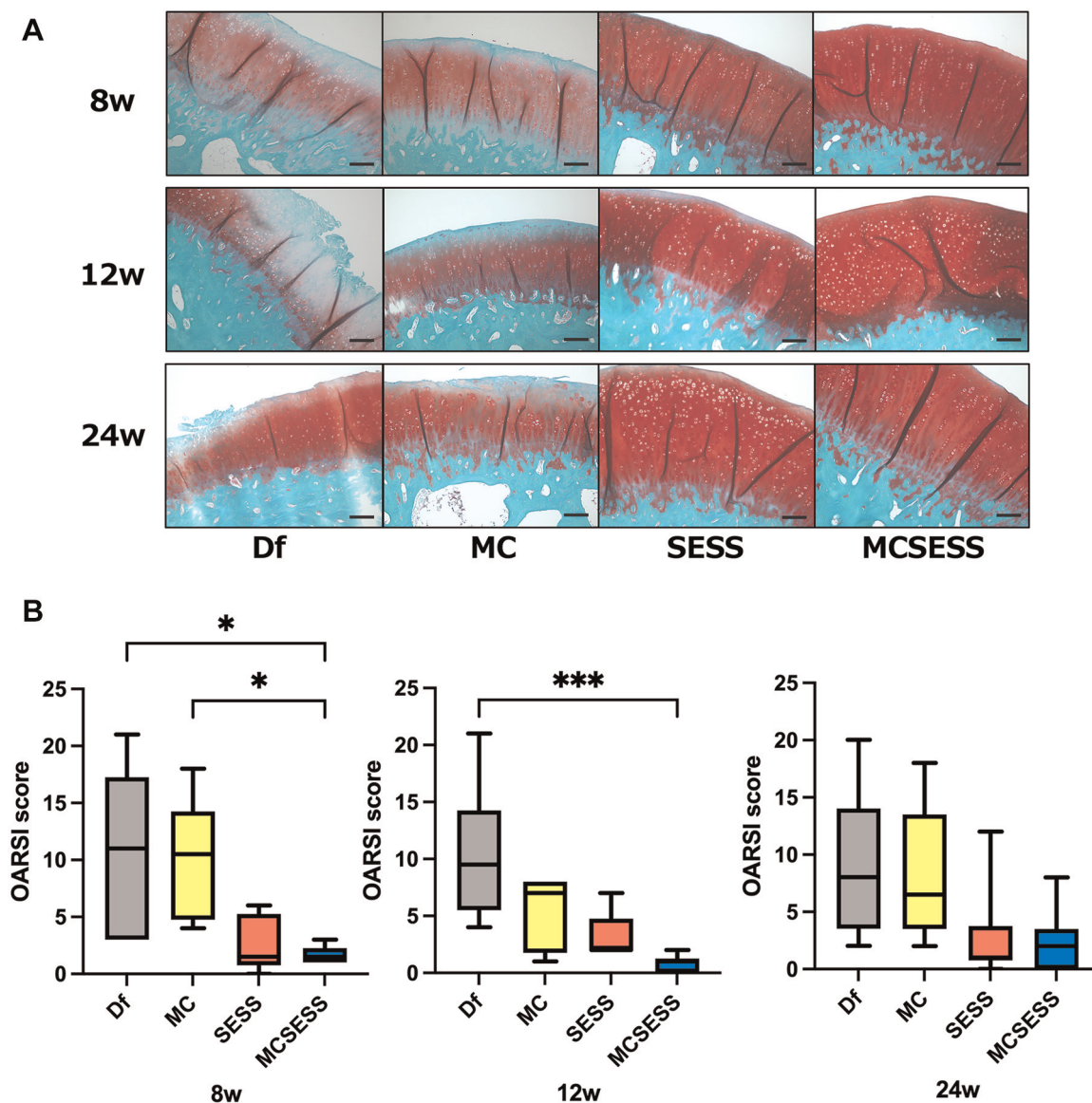


Figure 5. (A) Safranin O/Fast Green staining for the patella in each group at 8, 12, and 24 weeks postoperation. Scale bar: 300 mm. (B) OARSI scores in each group at 8, 12, and 24 weeks postoperation. * $P < .05$; *** $P < .001$. Df, defect; MC, minced cartilage; MCSESS, minced cartilage and silk-elastin and SpheroSeev; SESS, silk-elastin and SpheroSeev.

and MCSESS groups exhibited significantly higher than the Df group (Df vs SESS, $P = .029$, Df vs MCSESS, $P = .027$) (Table 2).

Moreover, Ki67 immunohistochemical analysis was performed at 8 weeks after surgery to evaluate cell proliferation. Ki67-positive cells were observed in all groups, with higher numbers in the SESS and MCSESS groups compared with the Df and MC groups (Figure 8A). The mean percentages of Ki67-positive cells in the Df, MC, SESS, and MCSESS groups were $8.9\% \pm 7\%$, $19.2\% \pm 10.5\%$, $31.8\% \pm 10.7\%$, and $32.8\% \pm 9.5\%$, respectively (Table 2). The percentage of Ki67-positive cells was significantly higher in the SESS and MCSESS groups than in the Df group (Df vs SESS, $P = .011$, Df vs MCSESS, $P = .0093$) (Figure 8B).

Although no significant differences were observed between the MC, SESS, and MCSESS groups, the SESS and MCSESS groups tended to have higher values.

DISCUSSION

This study focused on the comparative evaluation of each treatment group for osteochondral defect repair over 24 weeks. At the 24-week mark, the MCSESS and SESS groups demonstrated superior surface quality and integration with adjacent cartilage compared with the other groups. This suggests that the SESS mixture may enhance the structural and compositional quality of the repaired tissue.

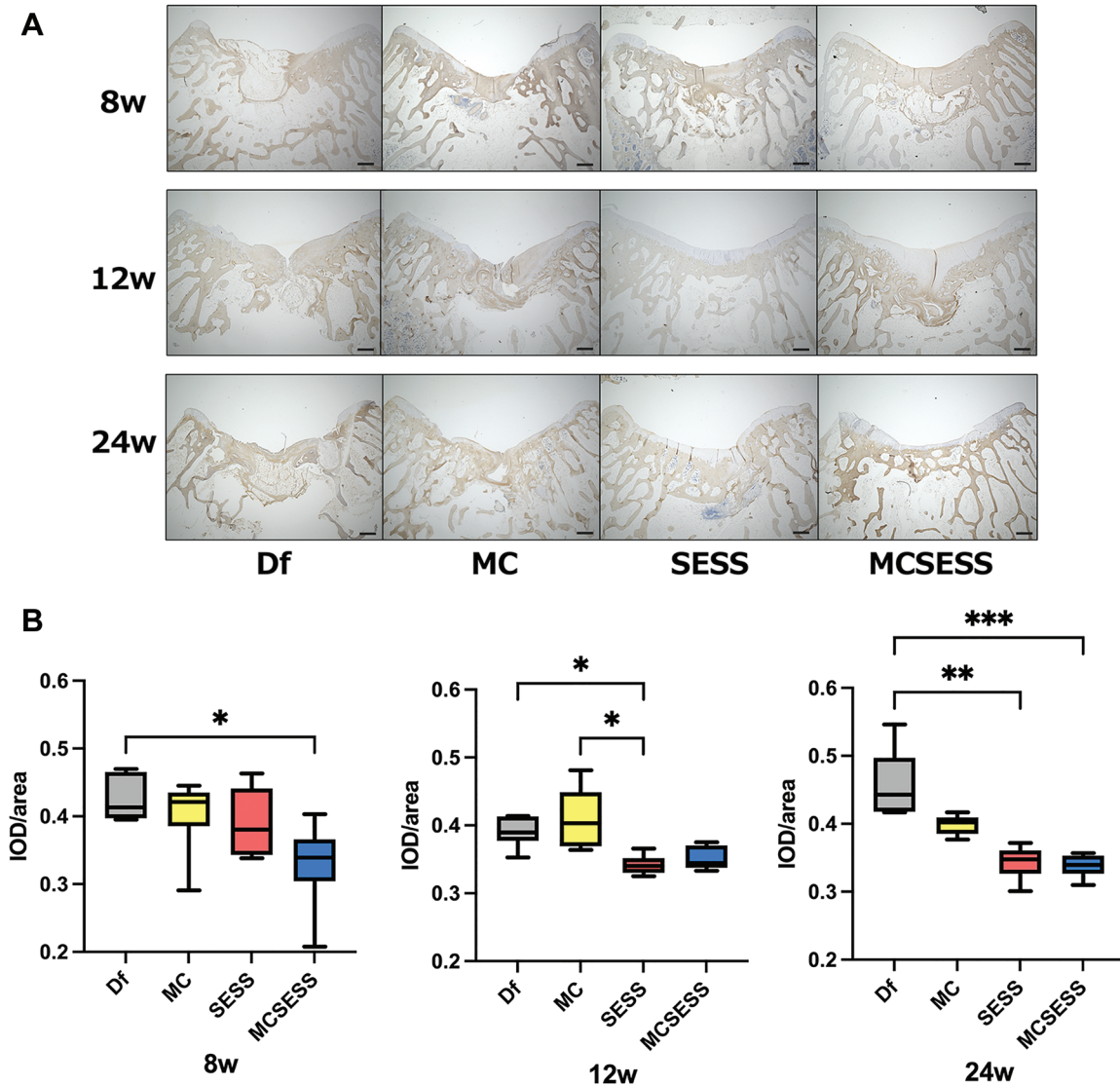


Figure 6. (A) Immunohistochemistry of COL1 in each group at 8, 12, and 24 weeks after surgery. Scale bar: 500 μ m. (B) The mean ratio of the IOD to area (IOD/area) was used to semi-quantify Col1. * $P < .05$; ** $P < .01$; *** $P < .001$. COL1, type I collagen; Df, defect; IOD, integrated optical density; MC, minced cartilage; MCSESS, minced cartilage and silk-elastin and SpheroSeev; SESS, silk-elastin and SpheroSeev.

The novelty of this study lies in the combination of a silk-elastin sponge, which is clinically used for skin ulcer treatment,²⁸ with SpheroSeev. SpheroSeev is known for its flexibility, elasticity, biocompatibility, and sustained cell activity, indicating its potential for osteochondral defect repair. In comparison with other cartilage repair studies using the Modified O'Driscoll histological scoring scale, Getgood et al¹¹ reported scores of 16.83 for recombinant human fibroblast growth factor 18 (rhFGF18) at 24 weeks in an ovine model utilizing a biphasic collagen/glycosaminoglycans scaffold with rhFGF18 or BMP-7. Frenkel et al¹⁰ compared 2 different biphasic implants in a rabbit osteochondral defect model and reported scores of 20.4 for a polyelectrolytic complex hydrogel of hyaluronic acid and chitosan and 19.1 for type I collagen at 24 weeks. In

addition, Demir et al¹⁴ reported scores of 15.2 for Chondro-Gide, 16.2 for MaioRegen, and 19.7 for poly-D, L-lactide-co-caprolactone at 12 weeks in a rabbit osteochondral defect model comparing 3 cell-free matrix scaffolds. Consistent with these findings, the SESS group (20.7) and the MCSESS group (20.3) showed comparable cartilage repair effects in this study. Furthermore, the mean percentages of Ki67-positive cells in the subchondral bone for the Df, MC, SESS, and MCSESS groups were $8.9\% \pm 7\%$, $19.2\% \pm 10.5\%$, $31.8\% \pm 10.7\%$, and $32.8\% \pm 9.5\%$, respectively. The significance of cell proliferation in subchondral bone for cartilage repair has been demonstrated in several studies using rabbit models. Wu et al³⁸ suggested that the activation of progenitor cells and bone marrow stem cells in the subchondral bone is crucial for the

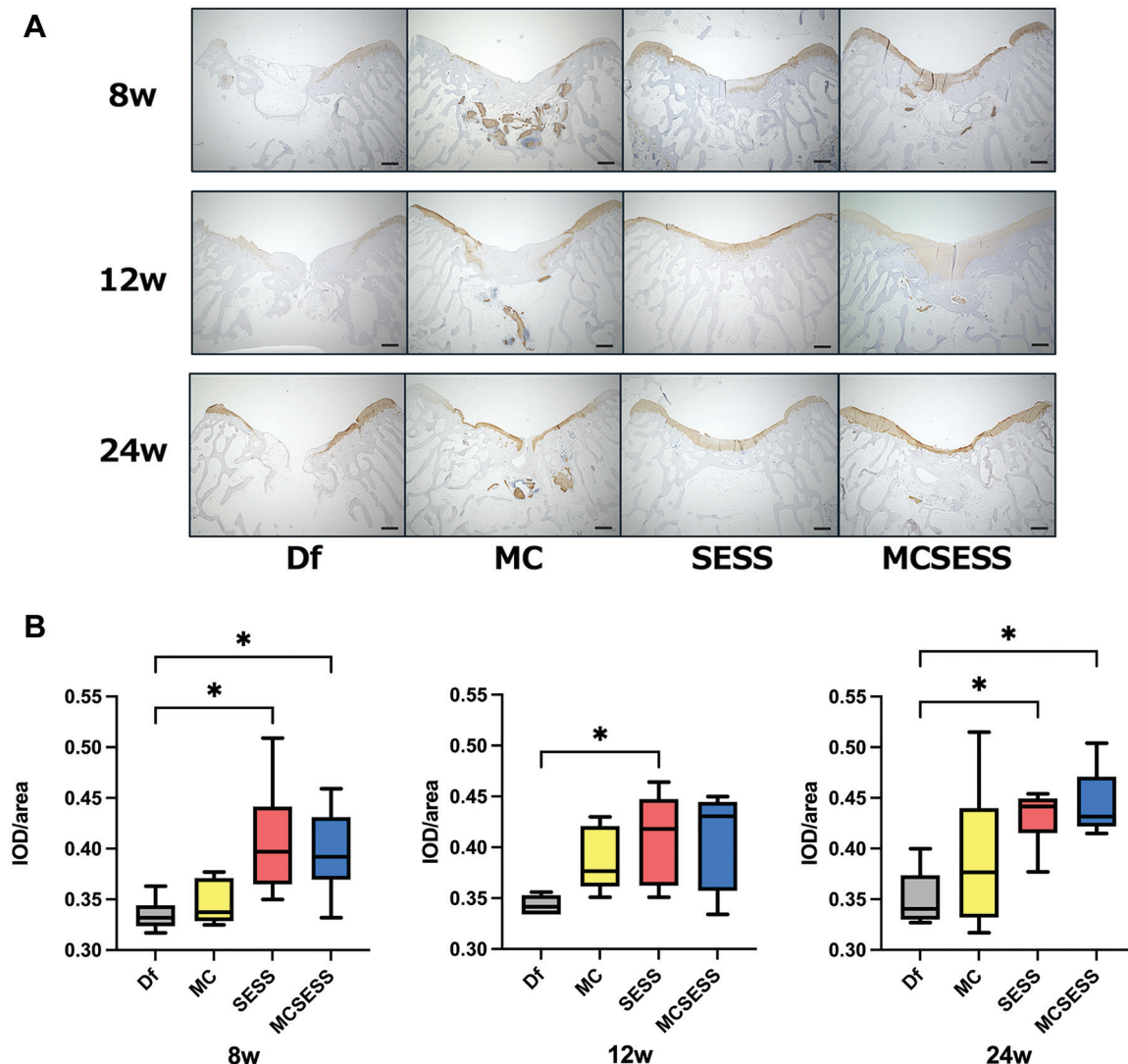


Figure 7. (A) Immunohistochemistry of COLII in each group at 8, 12, and 24 weeks postoperation. Scale bar: 500 μ m. (B) The mean ratio of IOD to area (IOD/area) was used to semi-quantify COLII. * $P < .05$. COLII, type II collagen; Df, defect; IOD, integrated optical density; MC, minced cartilage; MCSESS, minced cartilage and silk-elastin and SpheroSeev; SESS, silk-elastin and SpheroSeev.

repair and remodeling of subchondral bone in a collagenase-induced temporomandibular joint osteoarthritis rabbit model. Wang et al³⁷ evaluated the repair response 1 year after implanting an allogenic periosteum-derived cell polylactic acid composite graft in the femoral condyle osteochondral defect of New Zealand White rabbits, highlighting the importance of healthy subchondral bone for joint cartilage repair. The elevated Ki67 expression in subchondral bone indicates active tissue remodeling and vascular formation, which supports the cartilage repair process through multiple mechanisms. This finding aligns with current understanding of osteochondral repair as a coordinated process involving both bone and cartilage compartments.¹⁵ Our results showed that MC alone demonstrated inferior cartilage repair compared with SESS and MCSESS. This aligns with the findings of Andjelkov

et al¹ that without scaffolds, cartilage repair is poor because of the lack of chemo-tactical, mechano-tactical, and electro-tactical factors necessary for mesenchymal stem cell-like fibroblast migration. Consistent with a previous study,²⁶ these findings suggest that scaffolds play a significant role in cartilage repair.

Our study also found that the cartilage in the patella, which is in contact with the osteochondral defect site on the femoral trochlea, showed slower degeneration with SESS compared with the Df group. This finding suggests that SESS may help prevent cartilage degeneration in regions not directly affected by osteochondral defects. Although there are a few reports directly correlating patellar cartilage degeneration with femoral cartilage repair, Koh et al¹⁹ investigated the contact pressure resulting from mismatched grafts in osteochondral defects of the

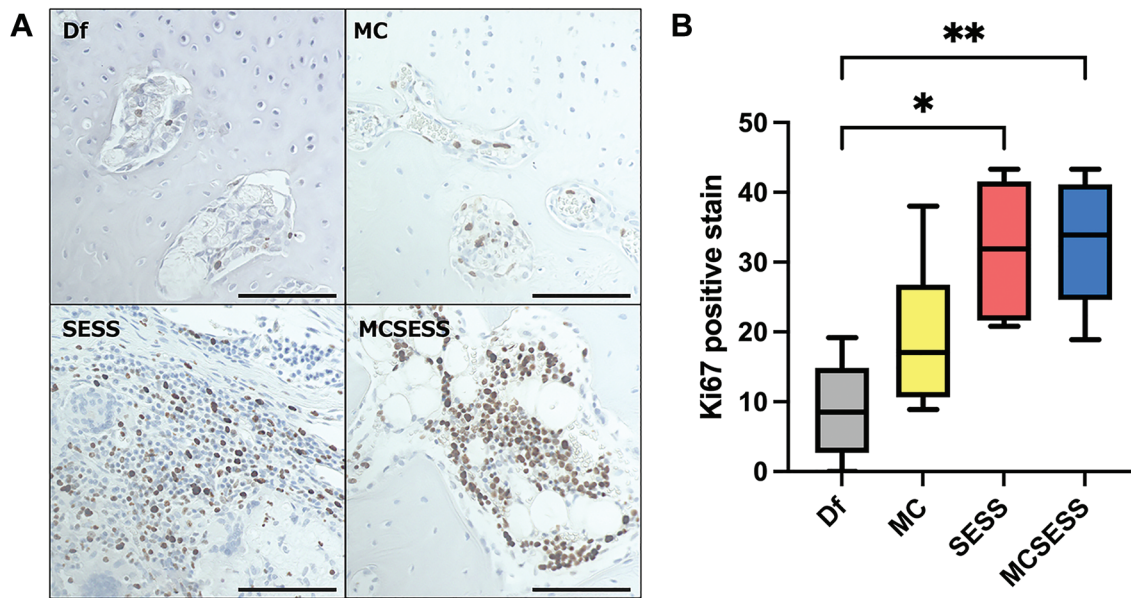


Figure 8. (A) Immunohistochemistry of Ki67 in each group at 8 weeks postoperatively. Scale bar: 100 μ m. (B) The rate of Ki67-positive cells in the reparative tissue in the subchondral bone. * $P < .05$; ** $P < .01$. Df, defect; MC, minced cartilage; MCSESS, minced cartilage and silk-elastin and SpheroSeev; SESS, silk-elastin and SpheroSeev.

medial femoral condyle. They reported that contact pressure increased with defects or mismatched grafts compared with normal cartilage, potentially exacerbating adjacent cartilage degeneration.¹¹ Other studies have similarly indicated that mismatched defects can adversely affect adjacent cartilage.^{12,13,20} Our results suggest that sustained mismatched defects may lead to increased contact pressure and subsequent cartilage degeneration.

The novelty of our study lies in the observation that SESS not only promotes osteochondral defect repair but also exerts a protective effect on adjacent cartilage, such as the patella, by maintaining scaffold integrity. The ability of SESS to mitigate cartilage degeneration indirectly related to the defect highlights its potential as a comprehensive treatment option for osteochondral injuries and offers a new perspective on preventing the progression of osteoarthritis.

In addition, there were no significant differences in cartilage repair between the SESS and MCSESS groups. Considering the simplicity of the technique and consistency with the findings of Demir et al that indicated cell-free scaffolds alone were effective in cartilage repair, SESS alone might be sufficient for achieving cartilage repair.¹⁴ Future studies should investigate the use of SESS in larger animal models to better understand its potential for clinical translation and evaluate its long-term effects on both cartilage repair and adjacent structures.

Limitations

This study has a few limitations. First, further investigation is needed to determine whether SESS is superior to other

scaffolds in treating osteochondral defects. Matsiko et al²⁶ emphasized the importance of scaffold microstructure, showing that larger pore sizes promote cartilage formation, gene expression, and matrix deposition. However, the microstructure of SESS is not well defined and requires further research. Second, although this study used Japanese White rabbits and did not observe obvious complications, such as infections, arthritis, or rapid disease progression, more cautious research is necessary before the clinical application of SESS in humans. Similar to this limitation, our study used small animal models (rabbits), which possess a higher regenerative potential than humans. The results observed, particularly with subchondral repair, may not directly translate to human patients because of differences in healing capacity. Last, the detailed mechanism by which SESS achieves effective tissue repair remains unclear. The effects of SESS on chondrocyte migration, proliferation, integration with surrounding tissues, and remodeling need further elucidation. Despite these limitations, the use of SESS for scaffold creation holds the potential to simplify future osteochondral defect treatments.

CONCLUSION

The combination of silk-elastin, SpheroSeev, and MC as scaffolds may enhance cartilage repair in osteochondral defects in rabbits. Notably, the SESS mixture demonstrates promising potential for improving the structural integrity and biochemical composition of repaired tissue, suggesting an effective approach for addressing osteochondral defects.


ACKNOWLEDGMENT

The authors are indebted to Dr Goki Kamei and Dr Junya Tsukisaka for their significant contributions to the histological score evaluation. The authors also acknowledge Sanyo Chemical Industries, Ltd, for providing the silk-elastin and Seevix for providing the SpheroSeev.

ORCID iDs

Naofumi Hashiguchi  <https://orcid.org/0000-0002-3029-2599>

Masakazu Ishikawa  <https://orcid.org/0000-0002-8561-6028>

Atsuo Nakamae  <https://orcid.org/0000-0003-0449-9083>

REFERENCES

- Andjelkov N, Riyadh H, Ivarsson M, Kacarevic-Popovic Z, Krstic J, Wretenberg P. The enhancement of cartilage regeneration by use of a chitosan-based scaffold in a 3D model of microfracture in vitro: a pilot evaluation. *J Exp Orthop*. 2021;8(1):12.
- Biant LC, Bentley G, Vijayan S, Skinner JA, Carrington RWJ. Long-term results of autologous chondrocyte implantation in the knee for chronic chondral and osteochondral defects. *Am J Sports Med*. 2014;42(9):2178-2183.
- Bonasia DE, Marmotti A, Mattia S, et al. The degree of chondral fragmentation affects extracellular matrix production in cartilage autograft implantation: an in vitro study. *Arthroscopy*. 2015;31(12):2335-2341. PMID: 26321111
- Chen Z, Zhang Q, Li H, Wei Q, Zhao X, Chen F. Elastin-like polypeptide modified silk fibroin porous scaffold promotes osteochondral repair. *Bioact Mater*. 2021;6(3):589-601. PMID: 33005824
- Cole BJ, DeBerardino T, Brewster R, et al. Outcomes of autologous chondrocyte implantation in the study of the treatment of articular repair (STAR) patients with osteochondritis dissecans. *Am J Sports Med*. 2012;40(9):2015-2022.
- Cole BJ, Farr J, Winalski CS, et al. Outcomes after a single-stage procedure for cell-based cartilage repair: a prospective clinical safety trial with 2-year follow-up. *Am J Sports Med*. 2011;39(6):1170-1179.
- Cvetanovich GL, Riboh JC, Tilton AK, Cole BJ. Autologous chondrocyte implantation improves knee-specific functional outcomes and health-related quality of life in adolescent patients. *Am J Sports Med*. 2017;45(1):70-76.
- Farokhi M, Mottaghtalab F, Fatahi Y, et al. Silk fibroin scaffolds for common cartilage injuries: possibilities for future clinical applications. *Eur Polym J*. 2019;115:251-267.
- Foldager CB. Advances in autologous chondrocyte implantation and related techniques for cartilage repair. *Dan Med J*. 2013;60(4):B4600. PMID: 23651721
- Frenkel SR, Bradica G, Brekke JH, et al. Regeneration of articular cartilage—evaluation of osteochondral defect repair in the rabbit using multiphasic implants. *Osteoarthritis Cartilage*. 2005;13(9):798-807.
- Getgood A, Henson F, Skelton C, et al. Osteochondral tissue engineering using a biphasic collagen/GAG scaffold containing rhFGF18 or BMP-7 in an ovine model. *J Exp Orthop*. 2014;1(1):13.
- Gilat R, Haunschild ED, Knapik DM, Cole BJ. Single-stage minced autologous cartilage restoration procedures. *Oper Tech Sports Med*. 2020;28(4):150782.
- Hakimi O, Knight DP, Vollrath F, Vadgama P. Spider and mulberry silkworm silks as compatible biomaterials. *Composites Part B*. 2007;38(3):324-337.
- Irem Demir A, Pulatkan A, Ucan V, et al. Comparison of 3 cell-free matrix scaffolds used to treat osteochondral lesions in a rabbit model. *Am J Sports Med*. 2022;50(5):1399-1408.
- Jiang J, Nicoll SB, Lu HH. Co-culture of osteoblasts and chondrocytes modulates cellular differentiation in vitro. *Biochem Biophys Res Commun*. 2005;338(2):762-770. PMID: 16259947
- Katsube K, Ochi M, Uchio Y, et al. Repair of articular cartilage defects with cultured chondrocytes in atelocollagen gel. Comparison with cultured chondrocytes in suspension. *Arch Orthop Trauma Surg*. 2000;120(3-4):121-127. PMID: 10738867
- Kawabata S, Kanda N, Hirasawa Y, et al. The utility of silk-elastin hydrogel as a new material for wound healing. *Plast Reconstr Surg Glob Open*. 2018;6(5):e1778. PMID: 29922560
- Kim DK, In Kim J, Sim BR, Khang G. Bioengineered porous composite curcumin/silk scaffolds for cartilage regeneration. *Mater Sci Eng C Mater Biol Appl*. 2017;78:571-578. PMID: 28576023
- Koh JL, Wirsing K, Lautenschlager E, Zhang LO. The effect of graft height mismatch on contact pressure following osteochondral grafting: a biomechanical study. *Am J Sports Med*. 2004;32(2):317-320. PMID: 14977653
- Latt LD, Glisson RR, Montijo HE, Usulli FG, Easley ME. Effect of graft height mismatch on contact pressures with osteochondral grafting of the talus. *Am J Sports Med*. 2011;39(12):2662-2669. PMID: 21937745
- Lavery S, Girard CA, Williams JM, Hunziker EB, Pritzker KPH. The OARS histopathology initiative—recommendations for histological assessments of osteoarthritis in the rabbit. *Osteoarthritis Cartilage*. 2010;18(suppl 3):S53-S65. PMID: 20864023
- Lefèvre T, Auger M. Spider silk as a blueprint for greener materials: a review. *Int Mater Rev*. 2016;61(2):127-153.
- Loncoñanco E, Navarrete F, Cuevas N, Vasconcellos A, Paredes M. Integrated optical density analysis of the immunohistochemical expression of the progesterone receptor in the uterine endometrium of prepubertal araucana sheep. *Int J Morphol*. 2021;39(5):1278-1282.
- Marmotti A, Bruzzone M, Bonasia DE, et al. One-step osteochondral repair with cartilage fragments in a composite scaffold. *Knee Surg Sports Traumatol Arthrosc*. 2012;20(12):2590-2601. PMID: 22349601
- Massen FK, Inauen CR, Harder LP, Runer A, Preiss S, Salzmann GM. One-step autologous minced cartilage procedure for the treatment of knee joint chondral and osteochondral lesions: a series of 27 patients with 2-year follow-up. *Orthop J Sports Med*. 2019;7(6):2325967119853773.
- Matsiko A, Gleeson JP, O'Brien FJ. Scaffold mean pore size influences mesenchymal stem cell chondrogenic differentiation and matrix deposition. *Tissue Eng Part A*. 2015;21(3-4):486-497. PMID: 25203687
- Matsushita R, Nakasa T, Ishikawa M, et al. Repair of an osteochondral defect with minced cartilage embedded in atelocollagen gel: a rabbit model. *Am J Sports Med*. 2019;47(9):2216-2224. PMID: 31206306
- Noda K, Kawai K, Matsuura Y, et al. Safety of silk-elastin sponges in patients with chronic skin ulcers: a phase I/II, single-center, open-label, single-arm clinical trial. *Plast Reconstr Surg Glob Open*. 2021;9(4):e3556. PMID: 33936917
- Ozaki C, Somamoto S, Kawabata S, Tabata Y. Effect of an artificial silk elastin-like protein on the migration and collagen production of mouse fibroblasts. *J Biomater Sci Polym Ed*. 2014;25(12):1266-1277. PMID: 24941248
- Perdisa F, Filardo G, Sessa A, et al. One-step treatment for patellar cartilage defects with a cell-free osteochondral scaffold: a prospective clinical and MRI evaluation. *Am J Sports Med*. 2017;45(7):1581-1588. PMID: 28263667
- Rutgers M, van Pelt MJP, Dhert WJA, Creemers LB, Saris DBF. Evaluation of histological scoring systems for tissue-engineered, repaired, and osteoarthritic cartilage. *Osteoarthritis Cartilage*. 2010;18(1):12-23. PMID: 19747584
- Salehi S, Koeck K, Scheibel T. Spider silk for tissue engineering applications. *Molecules*. 2020;25(3):737. PMID: 32046280

33. Salzmänn GM, Ossendorff R, Gilat R, Cole BJ. Autologous minced cartilage implantation for treatment of chondral and osteochondral lesions in the knee joint: an overview. *Cartilage*. 2021;13(suppl 1):S1124-S1136. PMID: 32715735
34. Stern-Tal D, Ittah S, Sklan E. A new cell-sized support for 3D cell cultures based on recombinant spider silk fibers. *J Biomater Appl*. 2022;36(10):1748-1757.
35. Tsuyuguchi Y, Nakasa T, Ishikawa M, et al. The benefit of minced cartilage over isolated chondrocytes in atelocollagen gel on chondrocyte proliferation and migration. *Cartilage*. 2021;12(1):93-101. PMID: 30311776
36. Vijayan S, Bentley G, Briggs T, et al. Cartilage repair: a review of Stanmore experience in the treatment of osteochondral defects in the knee with various surgical techniques. *Indian J Orthop*. 2010;44(3):238-245. PMID: 20697474
37. Wang HC, Lin TH, Hsu CC, Yeh ML. Restoring osteochondral defects through the differentiation potential of cartilage stem/progenitor cells cultivated on porous scaffolds. *Cells*. 2021;10(12):3536.
38. Wu G, Zhu S, Sun X, Hu J. Subchondral bone changes and chondrogenic capacity of progenitor cells from subchondral bone in the collagenase-induced temporomandibular joints osteoarthritis rabbit model. *Int J Clin Exp Pathol*. 2015;8(9):9782-9789.
39. Zhao W, Zou T, Cui H, et al. Parathyroid hormone (1-34) promotes the effects of 3D printed scaffold-seeded bone marrow mesenchymal stem cells on meniscus regeneration. *Stem Cell Res Ther*. 2020;11(1):328. PMID: 32731897